



Budapest University of Technology and Economics
Department of Networked Systems and Services
Laboratory of Acoustics and Studio Technologies
H-1117 Budapest, 2. Magyar tudósok körútja

Phone: (+36-1) 463-2543
Fax: (36-1) 463-3263
E-mail: rucz@hit.bme.hu
URL: <http://last.hit.bme.hu>

Acoustical analysis of innovative flute heads

Official report

Prepared by: Péter Rucz, Ph.D.



April 28, 2017
Budapest

1 Details of the analysis

1.1 Objectives

The purpose of the analysis introduced in this report is to describe the acoustical features of the innovative flute head invented by the Customer. The detailed examination is based on objective measurements and the results are compared with the features of traditional flute heads. In the investigations reported here different notes produced by flutes both with a traditional head and with the innovative flute heads were examined. These sounds and vibrations were recorded using calibrated measurement instruments and analysed utilizing the methods described below.

1.2 Environment

- Budapest University of Technology and Economics, Department of Networked Systems and Services (HIT), Laboratory of Acoustics and Studio Technologies, semi-anechoic chamber (H1117 Budapest, 2 Magyar tudósok körútja, room IE222).
- Date and time: January 17, 2017, 11:00–17:00 CET; March 7, 2017, 11:00–17:00 CET
- Temperature: 23.5–25.0 °C
- Participants: Zoltán Lakat (flautist), Péter Rucz (electrical engineer)

1.3 Equipment

- Trevor James Cantabile flute, equipped with: a traditional tuning plug, and several other tuning plugs made of steel, cocobolo, bone, silver or titanium
- Condenser microphones: 4 pieces, type TMS 130P10 1/4" (nominal sensitivity: 20 mV/Pa)
- Accelerometers: 2 pieces, type PCB 353B13 (nominal sensitivity: 5.1 mV/g)
- Sound pressure level calibrator: Larson–Davis CAL250
- Measurement amplifier: PCB 482A20
- Data collection module: NI9234
- Laptop computer: HP ProBook with NiHu.Lab software

1.4 Recordings

Six different head joints were used in the measurement: flutes equipped with a new steel, cocobolo, bone, silver or titanium tuning plug, and a flute with a traditional head. Sounds produced by these six different flute sets were recorded and stored. Recordings were made in the full musical scale playable on the flute—from c' (one-lined c , further referred to as C1) to c'''' (four-lined c , further referred to as C4)—playing the notes *piano* and *forte*, one by one, in a sequence along the chromatic scale. Altogether $6 \times 37 \times 2 = 444$ sound samples were recorded. In each sound sample the same note was sounded three times consecutively.¹

Sounds were converted to electric signals using the calibrated condenser microphones. The exact positions of the four microphones are marked with the numbers in circles in Figure 1. Microphone #1 was located at a distance of approx. 20 cm from the embouchure hole, while microphone #2 was positioned at a similar distance from the open end of the flute. Microphones #3 and #4 were placed at a distance of approx. 150 cm from the flautist, opposite and to the left hand side of the player, respectively.

¹Except for the note H3 played with the silver tuning plug—this sample contained only two sounds.

While recording vibrations, microphones #1 and #4 were replaced with the two accelerometers, whose positions are shown in Figure 2. Both accelerometers were fixed to the body of the flute using wax. Accelerometer #1 was placed close—approximately 2 cm—to the open end of the flute, while accelerometer #2 was placed close to the embouchure hole, approximately 5 cm from it. In case of vibration measurements, not all the notes of the chromatic scale were recorded, but only the following ones: C1, E1, G1, C2, E2, G2, C3, both with *piano* and *forte* dynamics. Signals from both the vibration sensors and the microphones were amplified and recorded using the same settings.

To achieve proper signal conditioning, the eight-channel PCB amplifier was used. The amplified signals were digitalized with a sampling frequency of $f_s = 51\,200$ Hz using the 24-bit four-channel data collection module NI9234. These digital samples were stored on the Laptop PC by the NiHu.Lab software for subsequent analysis. Beside the recorded samples, some notes were also made in order to facilitate the signal processing procedure and to mark certain samples for deletion.

Besides recording notes held long, repetitions of the same notes (C1, E1, G1, C2) were also recorded with each flute set. In the end the main theme from Ravel’s Bolero has been recorded for further analysis, also with each one of the six different flute heads.

2 Evaluation of the measurements

The measurements were evaluated in the following steps.

1. The data files containing the sound samples were loaded from NiHu.Lab and converted to a standard uncompressed audio format (`.wav`).
2. Based on the additional comments added to the sound samples, obsolete data was cut out.
3. Segmentation of the sound samples. First, the three successive sounds had to be detected in each sample. Then, the attack, steady state and decay phases were identified and marked in each sound. Results of the segmentation are visualized in Figure 3 for two example cases. The sound signals were filtered using a band-pass filter having a bandwidth of two octaves and a middle frequency defined as the nominal fundamental frequency of the corresponding musical note. The attack, steady state and decay phases were detected based on the temporal changes of the r.m.s. (root mean square) value of the filtered signals. Though this detection process was automated, its result was validated manually for each sound. This segmentation method was proven to be a valid choice for our analysis, as it yields proper detections even in case of very different sounds. The lower diagram of Figure 3 illustrates the segmentation process in case of the note H3 as an example. In case of the second (middle) sample the attack phase is much slower than in the first and the third samples; however, the automated segmentation process is able to handle this exceptional case properly.
4. As the next step the exact frequencies of the steady state sounds were evaluated. These exact frequencies were determined by extracting consecutive, fixed time windows from the steady state phase of the sounds. Frequencies detected by this method were used for calculating the average fundamental frequency and some of its other statistical measures (e.g. standard deviation or quartiles).
5. Once the exact fundamental frequency was determined, the sound samples were resampled. The new sampling frequency f'_s was chosen such that $f'_s = N f_1$, where N is an integer number ($N = 64$ in our case), and f_1 is the fundamental frequency. Thus, the spectral analysis could be performed on the resampled signals using coherent time windows and avoiding the spectral leakage and picket fence effects at the same time.



Figure 1: Measurement arrangement in the semi-anechoic chamber



Figure 2: Positions of the accelerometers on the flute

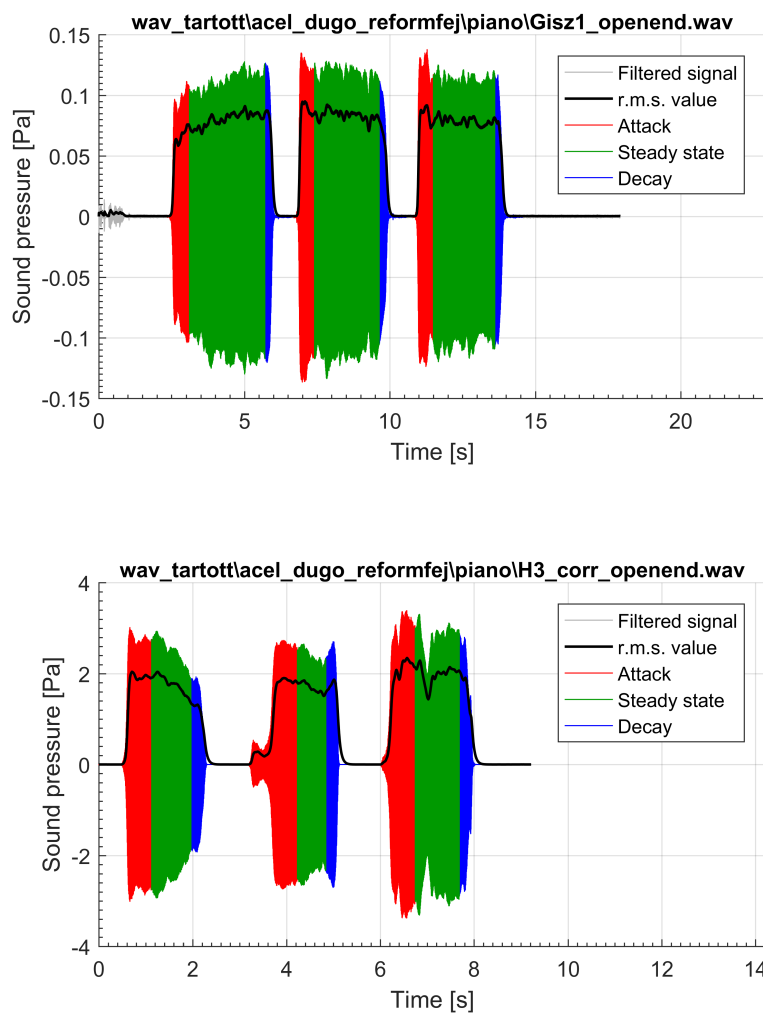


Figure 3: Results of the segmentation for two recorded sound samples. Top: steel plug, G#1, *piano*. Bottom: steel plug, H3, *piano*.

3 Analysis of notes held long

3.1 Analyzing the pitch

Evaluation of the pitch was performed on the steady state phases defined in the segmentation process. To be able to determine the fundamental frequency with a fine resolution, consecutive time windows were extracted from the steady state phase. Each time window consisted of $N_{\text{win}} = 8192$ samples and they were overlapping by $\text{ol} = 50\%$. In each time window the fundamental frequency was determined by modulation, low-pass filtering and harmonic fitting. Hence, the fundamental frequency was extracted with a time resolution of $T_{\text{win}} = N_{\text{win}}/f_s \cdot (1 - \text{ol}) \approx 0.08$ s. Depending on the length of the recorded sections, 10–200 time windows could be identified in the different steady state phases. (As more powerful blowing is necessary to produce and hold the notes in the upper register, steady state phases recorded there were significantly shorter.) An average of more than 100 time windows could be recorded along the whole range of the flute.

The frequencies measured in successive time windows are shown in Figure 4 for the six different flute sets. The pitches are displayed as errors compared to an imaginary tempered scale fitted to the average fundamental frequency of the notes using the method of least square mean errors. Each diagram shows the calculated differences compared to the fitted tempered scale. The thick horizontal line marks the average frequency in the diagrams, and the upper and lower edges show the upper and lower quartiles of the measured frequencies. The thin lines connecting the boxes and displayed above and below them visualize the minimum and the maximum of the measured frequency. The height of the boxes is proportional to the standard deviation of the frequency (assuming that the measured frequency has a normal distribution). A smaller box corresponds to a more stable pitch, while a higher box means a less stable pitch in the steady state. It is visible that the average frequency of the notes played with *piano* dynamics is below the tempered scale, while these values are above the scale in case of *forte* dynamics. This tendency corresponds well to our expectations. The phenomenon is explained by the fact that the sounding frequency of the flute depends on the blowing strength through the mouthpiece.

3.2 Analysis of sound pressure levels

Similarly to the analysis of the pitch, sound pressure levels were also calculated in the steady state phase. Sound pressure levels were evaluated based on the spectra calculated from the resampled sound signals. The resampled steady state signals were decomposed into different time windows using a window length of 4096 samples and an overlapping of 85%.² It is important to note that in this case—as a result of the resampling—the length of the windows varies based on the pitch. The decomposition gave over 100 time windows in the steady state phase in each case. Spectra were calculated on these time windows, weighted by the Hann window function. Sound pressure levels of the recorded sound samples were evaluated using these spectra.

The exact sensitivity of the microphones must be known in order to calculate sound pressure levels. The sensitivities were determined by a calibration process carried out prior to the measurements. Sound pressure levels of the recorded sound samples were calculated based on the spectrum by summing the power of the harmonics of the sound.³ The sound pressure level is given as the level of a signal having an r.m.s. value of p_{eff} expressed in units of dB SPL (sound pressure level) using the formula:

$$L \text{ [dB SPL]} = 20 \log_{10} \left(\frac{p_{\text{eff}}}{p_{\text{ref}}} \right), \quad \text{where } p_{\text{ref}} = 20 \mu\text{Pa}. \quad (1)$$

²This choice is supported by several earlier experiences. It was found earlier that spectrum calculations based on 4096 samples result in a sufficient frequency resolution. The 85% overlap is the observed upper limit, where noise repression due to averaging cannot be increased any further significantly.

³This way, the power of the broadband noise components of the sound are not included in the calculated sound pressure level. The analysis of the measured spectra confirmed that noise levels are at least 60 dB below the level of the signal. Therefore, the noise component does not have a significant influence on the sound pressure level.

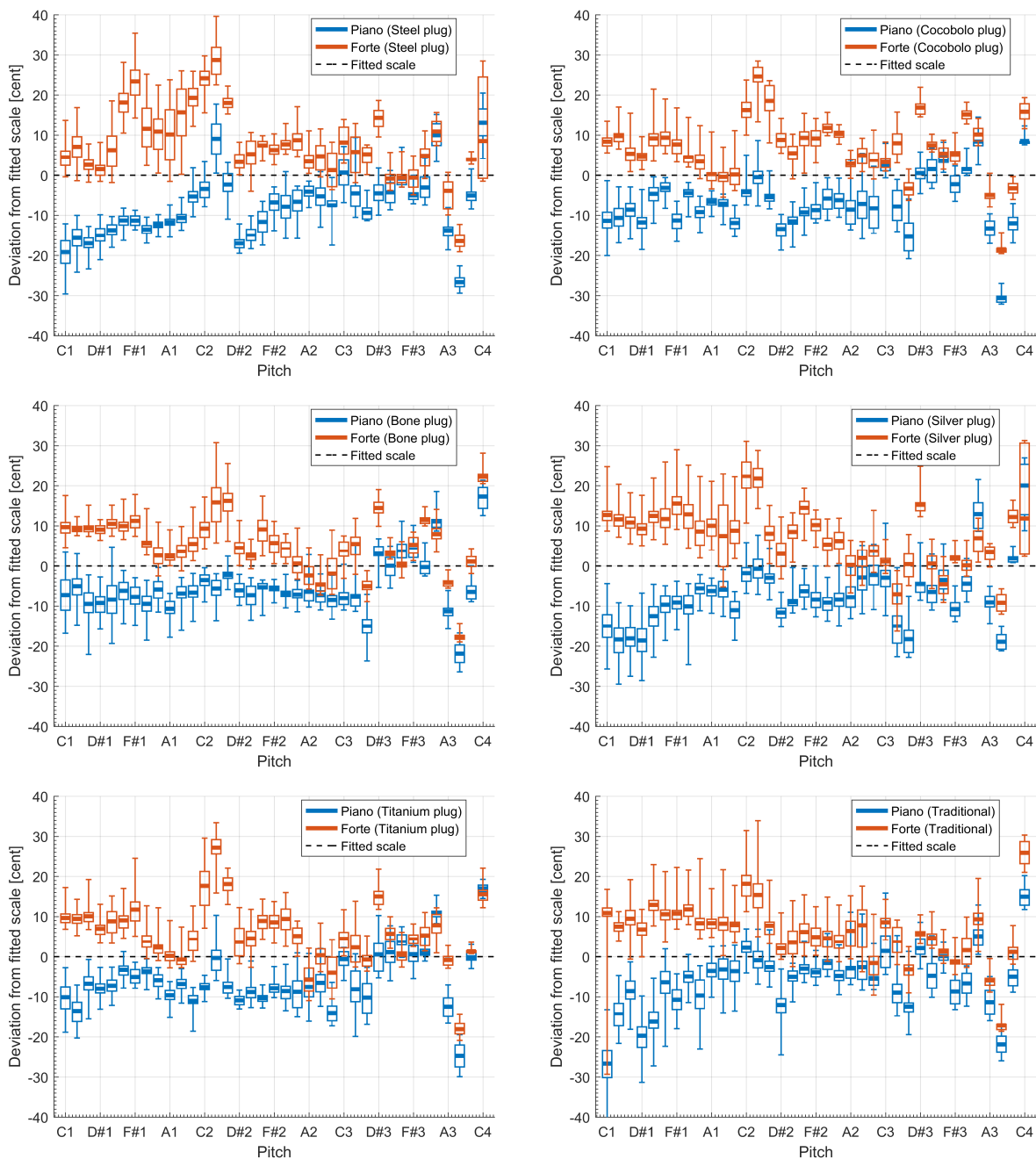


Figure 4: Measured frequency of notes held long over the full musical scale. Frequencies are plotted as deviations expressed in cents from a tempered scale fitted to the average frequencies using the method of minimal mean least square errors.

Figure 5 shows the average sound pressure levels of notes held long and played with *piano* (marked with blue on the chart) or *forte* (marked with red) dynamics. These sounds were recorded by microphone #2, close to the open end of the flute. The chart demonstrates that notes starting from D2 are played by overblowing that clearly increases the resulting sound pressure levels. As a result, there is a significant difference between the average sound pressure levels of the notes C#2 and D2 in each case.

Table 1 displays the average sound pressure levels measured when playing notes in *piano* and *forte* in the three-octave range of the flute. These sounds were produced by the six different flute sets and recorded separately. The whole musical range can be divided to three sub-ranges based

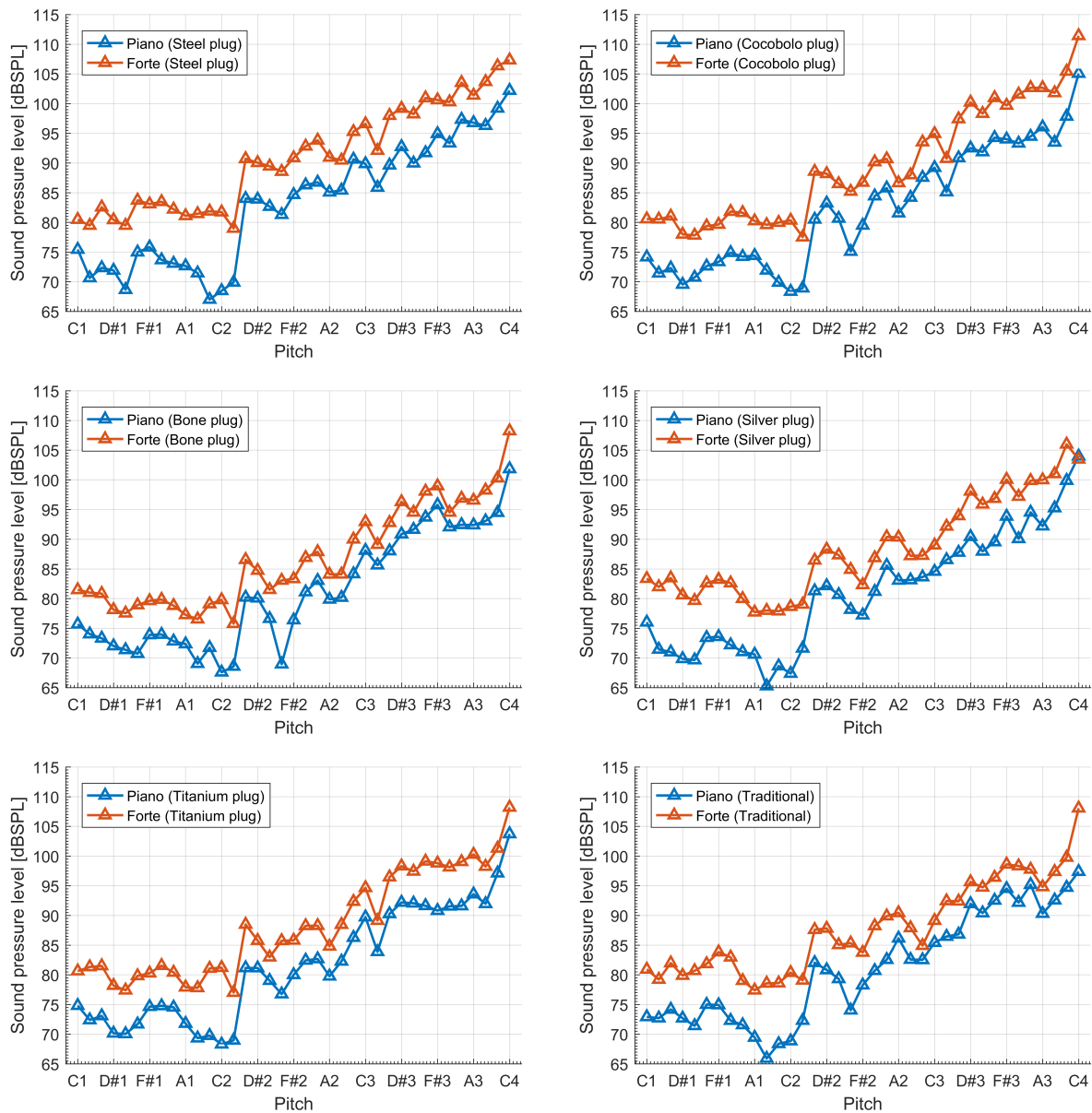


Figure 5: Measured sound pressure levels of the flutes with different head joints

Dynamics	Piano [dB SPL]			Forte [dB SPL]			F to P [dB]		
	Lower	Middle	Upper	Lower	Middle	Upper	Lower	Middle	Upper
Steel plug	72.2	85.9	95.7	81.5	92.1	102.3	9.3	6.2	6.6
Cocobolo plug	72.1	83.8	95.9	79.9	89.6	102.9	7.8	5.8	7.0
Bone plug	72.2	81.5	94.0	79.0	86.8	98.8	6.8	5.3	4.8
Silver plug	71.2	82.6	94.8	80.9	88.1	99.9	9.7	5.4	5.2
Titanium plug	72.0	82.8	94.4	79.9	88.5	100.2	7.8	5.7	5.9
Traditional plug	71.9	82.3	93.0	80.5	88.1	98.7	8.5	5.7	5.7

Table 1: Average sound pressure levels of notes held long played on different flutes measured near the open end over the three registers. Lower register: C1–C#2, Middle register: D2–C#3, Upper register: D3–C4. Column “F to P” means the *forte* to *piano* ratio.

on the amount of overblowing needed to produce the sounds. Lower register: C1–C#2, Middle register: D2–C#3, Upper register: D3–C4. Sound pressure levels displayed in the table are average dB SPL levels calculated for the three different registers. In the table the *forte* to *piano* ratio is also shown, which is the difference of the average levels of the notes played with *forte* and *piano* dynamics. Based on the data displayed in Table 1 the following conclusion can be drawn: sound pressure levels of notes played with different dynamics (*forte* or *piano*) in various registers are influenced by both the material and the type of the tuning plug. For example, the steel tuning plug enables higher levels in the middle and upper registers compared to the traditional plug when playing *forte* dynamics, while the levels of *piano* notes in the lower register are not affected significantly. Similar differences are observed when comparing the cocobolo and titanium tuning plugs with the traditional one. The *forte* to *piano* ratio is greater in case of both the silver and steel tuning plugs than that of the traditional plug, especially in case of sounds played in the lower register.

3.3 Analysis of the spectral centroid

The spectral centroid is a parameter which describes the timbre of the sound. If the spectral centroid value is higher, the timbre is richer in higher harmonics. If the spectral centroid value is lower, the fundamental is more dominant in the tone.

Spectral centroid is calculated as

$$C(X) = \frac{\sum_{n=1}^{N_{\text{harm}}} nX(nf_1)}{\sum_{n=1}^{N_{\text{harm}}} X(nf_1)}, \quad (2)$$

where C is the spectral centroid, X is the power spectrum of the signal, f_1 is the fundamental frequency, N_{harm} is the number of harmonics used in the calculation. In this analysis $N_{\text{harm}} = 10$ was chosen. According to formula (2) the spectral centroid is a dimensionless quantity, which can be converted to frequency by multiplying it by the fundamental frequency f_1 .

Diagrams of Figure 6 display the spectral centroid of held sounds, played *piano* and *forte* with the six different flute sets. In each case sounds were recorded at the open end of the flute. Great differences are observed of the spectral centroids of sounds played *piano* and *forte*. In case of notes played with *forte* dynamics the spectral centroid is significantly greater than in case of notes played with *piano* dynamics. In case of both dynamics there is a significant difference between the spectral centroid values of the notes played with different flute heads. In case of flutes with steel, cocobolo or titanium heads the spectral centroid of the produced notes is higher, thus their timbre is richer in higher harmonics compared to the traditional flute heads. The timbres of the held notes played with bone, silver and traditional plugs are similar. Average values of the spectral centroids per register are summarized in Table 2. It can also be noticed in Figure 6 that there are certain notes for each flute head whose spectral centroid differs significantly from that of the adjacent notes. In case of steel, cocobolo, bone, titanium and conventional tuning plugs such note is F2, while in case of the silver plug such notes are A#1 and F#2.

3.4 Analyzing the steady state spectrum

Steady state spectra of the notes C1–G1 produced by different flute heads with *piano* and *forte* dynamics are displayed in Figures 7–14. Based on former subjective evaluation, the spectra of the notes C1–G1 are expected to show the greatest differences, hence the choice of these notes. To facilitate the visual comparison of the charts, diagrams are drawn along the same horizontal and vertical scales. A normalized frequency scale is used in each diagram, with the value 1 corresponding to the fundamental frequency of each note. (Hence, the fundamental is always

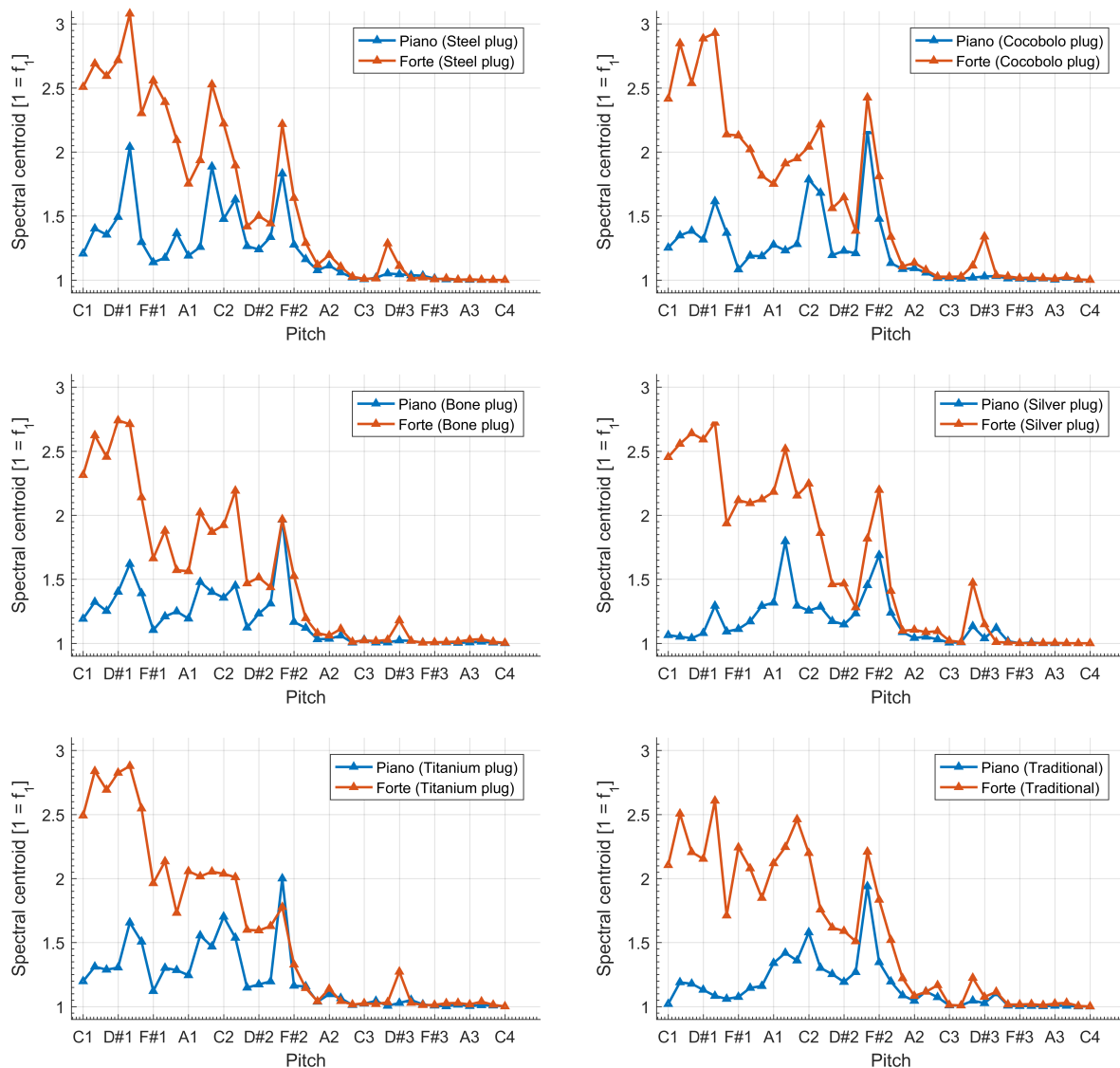


Figure 6: Spectral centroid in the full playable range with *piano* and *forte* dynamics

Dynamics	Piano			Forte		
	Lower	Middle	Upper	Lower	Middle	Upper
Steel plug	1.42	1.20	1.02	2.38	1.33	1.04
Cocobolo plug	1.36	1.22	1.01	2.26	1.38	1.05
Bone plug	1.33	1.17	1.01	2.12	1.28	1.03
Silver plug	1.22	1.18	1.03	2.30	1.34	1.06
Titanium plug	1.39	1.18	1.01	2.31	1.28	1.04
Traditional plug	1.22	1.21	1.02	2.16	1.41	1.05

Table 2: Average spectral centroids of the held notes played on different flute sets, measured at the open end of the flute over the three registers. Lower register: C1–C#2, Middle register: D2–C#3, Upper register: D3–C4.

represented by the nondimensional frequency 1 and harmonic partials correspond to the values 2, 3, 4 etc.) Steady state sound spectra of the sounds played *piano* are shown in the first and the second lines of the charts, while notes played *forte* are displayed in the third and fourth lines. Each figure shows the sound spectra for one certain note of the musical scale. In each case the average steady state amplitude spectrum of the three sounds is shown.

Sharp peaks representing the fundamental and the harmonic partials are observed in each case. Beside these sharp peaks wider peaks appear as well and become clearly visible typically at higher frequencies. These broader peaks correspond to the frequencies of natural resonance of the air column. The common features of these natural frequencies are the following. 1) In case of the first few harmonics, the sharp and broad peaks are very close to each other. Therefore it is very difficult or even impossible to distinguish the partials and the eigenfrequencies of the resonator. 2) At higher frequencies the broader eigenfrequency peaks are shifted from the peaks of the harmonics as the effective length of the air column is frequency dependent. This phenomenon is also called “stretching”. Stretching is visualized in the diagrams as well: harmonics and eigenfrequencies are well separable from the 4th or 5th harmonic partial in case of *piano* and from the 9th or 10th harmonics in case of *forte* dynamics. 3) The peaks corresponding to the eigenfrequencies become less sharp with increasing the frequency while their amplitude also decreases. This phenomenon is due to radiation losses at the openings and viscothermal losses occurring at the walls. It can be stated that the spectra displayed in the diagrams are in correspondence with the established and widely accepted physical model of the sound generation of the flute.

Differences between the sound spectra produced by the six different flute heads can also be observed in the charts. The summary below is not a full description of every little observable difference, rather it focuses on the main differences between the sound spectra of each note, describing these through a few representative examples. The main differences observed are as follows.

1. Significant change in the amplitude of a specific harmonic component can be observed when the note is played on flutes with different tuning plugs. In case of the note F1 (*piano*), for example, the amplitude of the second harmonic is significantly different when played with different plugs. The greatest difference is observable when comparing the cocobolo and the conventional tuning plugs and can be as high as 20 dB. In case of *forte* dynamics, similar differences can be observed when investigating the note G1.
2. When using different tuning plugs, the strongest partial of the note played can also change. Not only the strength of the harmonics change, but there are also alterations in the order of the amplitudes of the harmonic partials. An excellent example is the D#1 note, played with *forte* dynamics. When playing this note with a traditional tuning plug, the fundamental is the most dominant; however, in case of steel and silver plugs the octave is the most powerful component of the spectrum. With cocobolo, bone and titanium tuning plugs the second and the fourth harmonics have similar amplitudes.
3. Amplitudes of higher harmonic partials can change simultaneously. There are observable differences in the amplitudes of the higher (5th to 7th) partials, in case of the note G1, for example. Both with *piano* and *forte* dynamics, these harmonics appear with much greater amplitudes when played with the steel or cocobolo plugs. (This is in correspondence with the results shown in Figure 6 and Table 2.)

The perceived timbre is also affected by the alterations of the amplitudes of the different harmonics. Although there were no subjective experiments performed, it can be assumed that the above described objective differences do have an influence on the perceived sound quality of the flute.

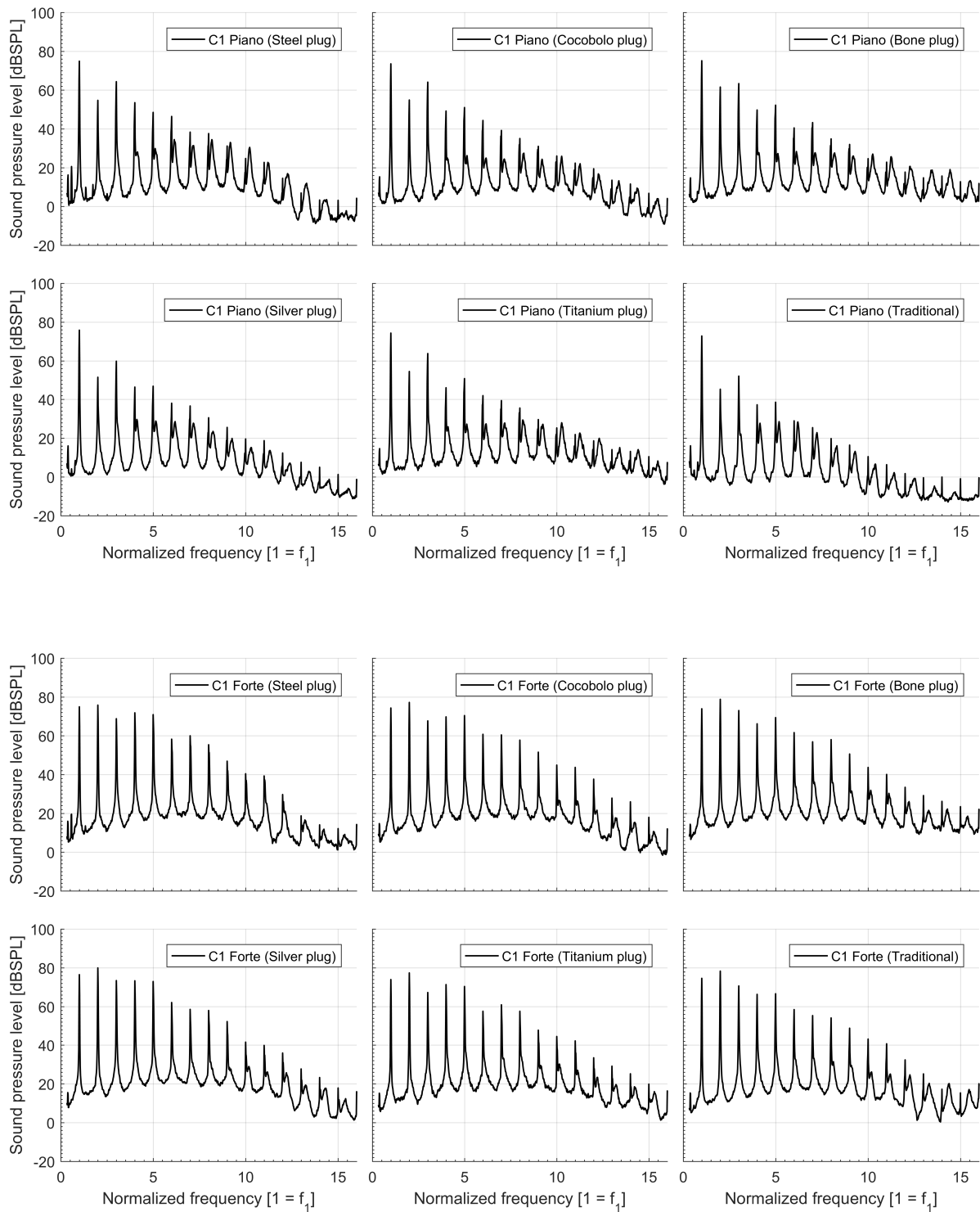


Figure 7: Steady state spectrum of the note C1 played with *piano* (first and second rows) and *forte* (third and fourth rows) dynamics on flutes with different head joints. (All diagrams have the same scale and shows the spectrum measured at the open end of the flute.)

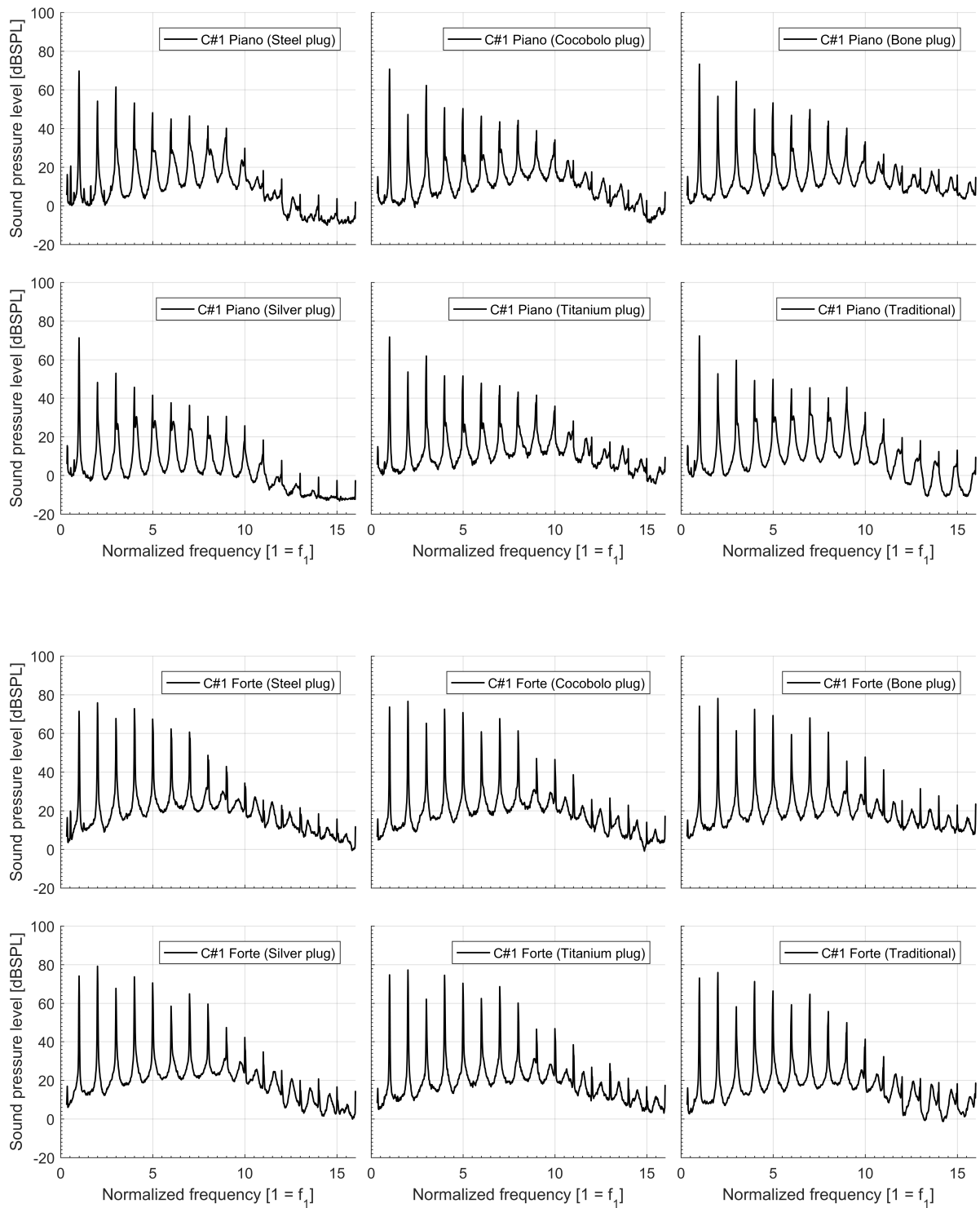


Figure 8: Steady state spectrum of the note C#1 played with *piano* (first and second rows) and *forte* (third and fourth rows) dynamics on flutes with different head joints. (All diagrams have the same scale and shows the spectrum measured at the open end of the flute.)

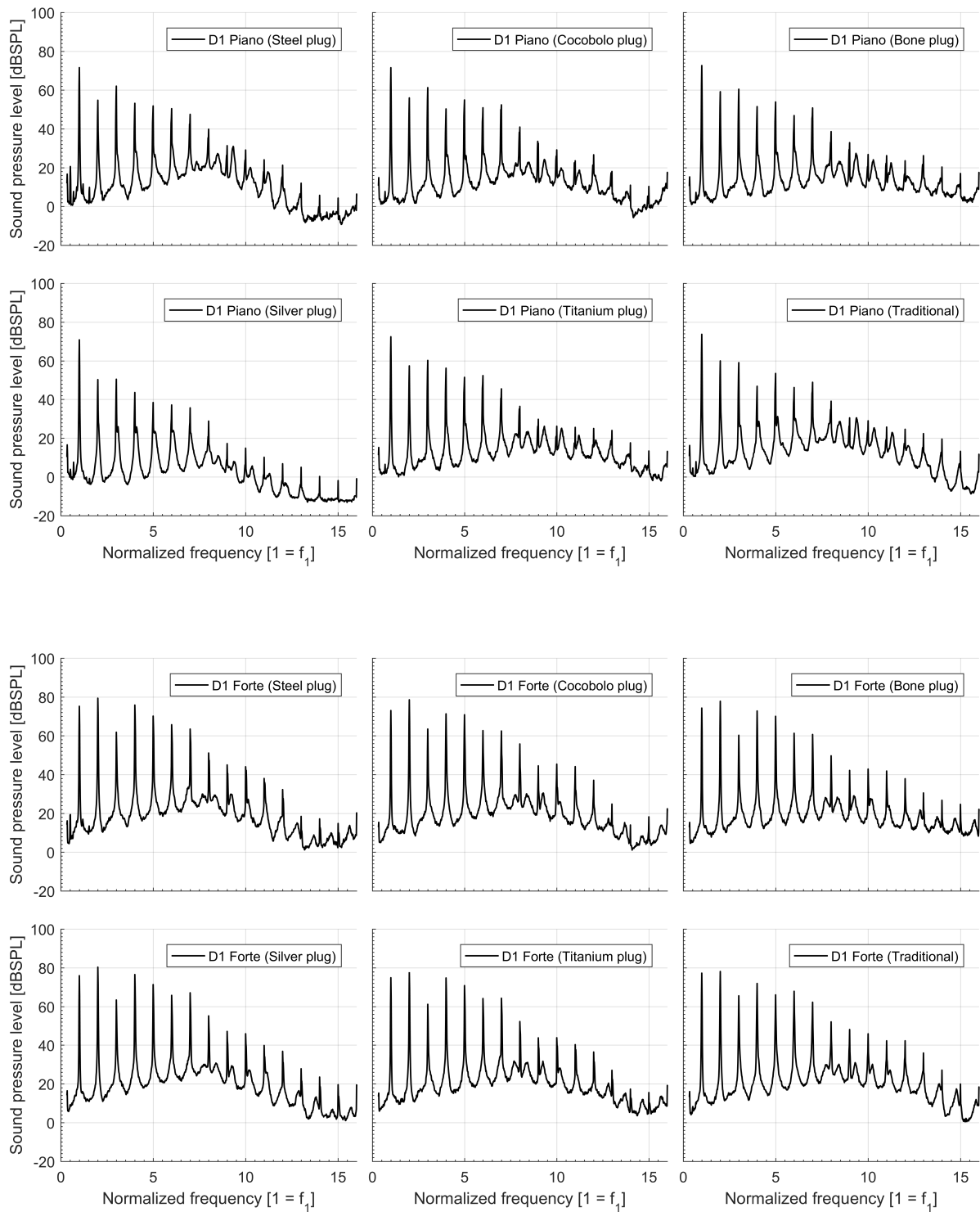


Figure 9: Steady state spectrum of the note D1 played with *piano* (first and second rows) and *forte* (third and fourth rows) dynamics on flutes with different head joints. (All diagrams have the same scale and shows the spectrum measured at the open end of the flute.)

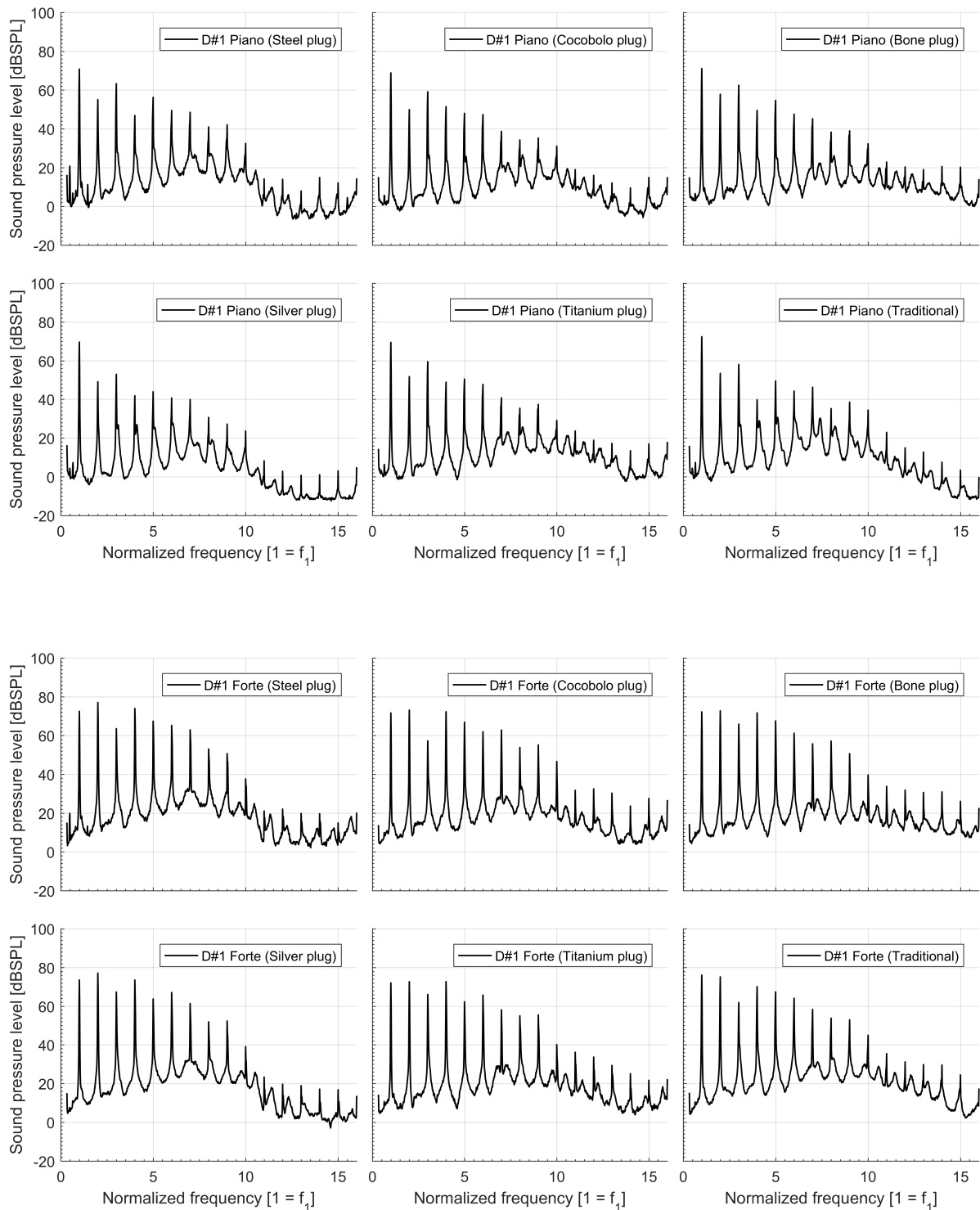


Figure 10: Steady state spectrum of the note D#1 played with *piano* (first and second rows) and *forte* (third and fourth rows) dynamics on flutes with different head joints. (All diagrams have the same scale and shows the spectrum measured at the open end of the flute.)

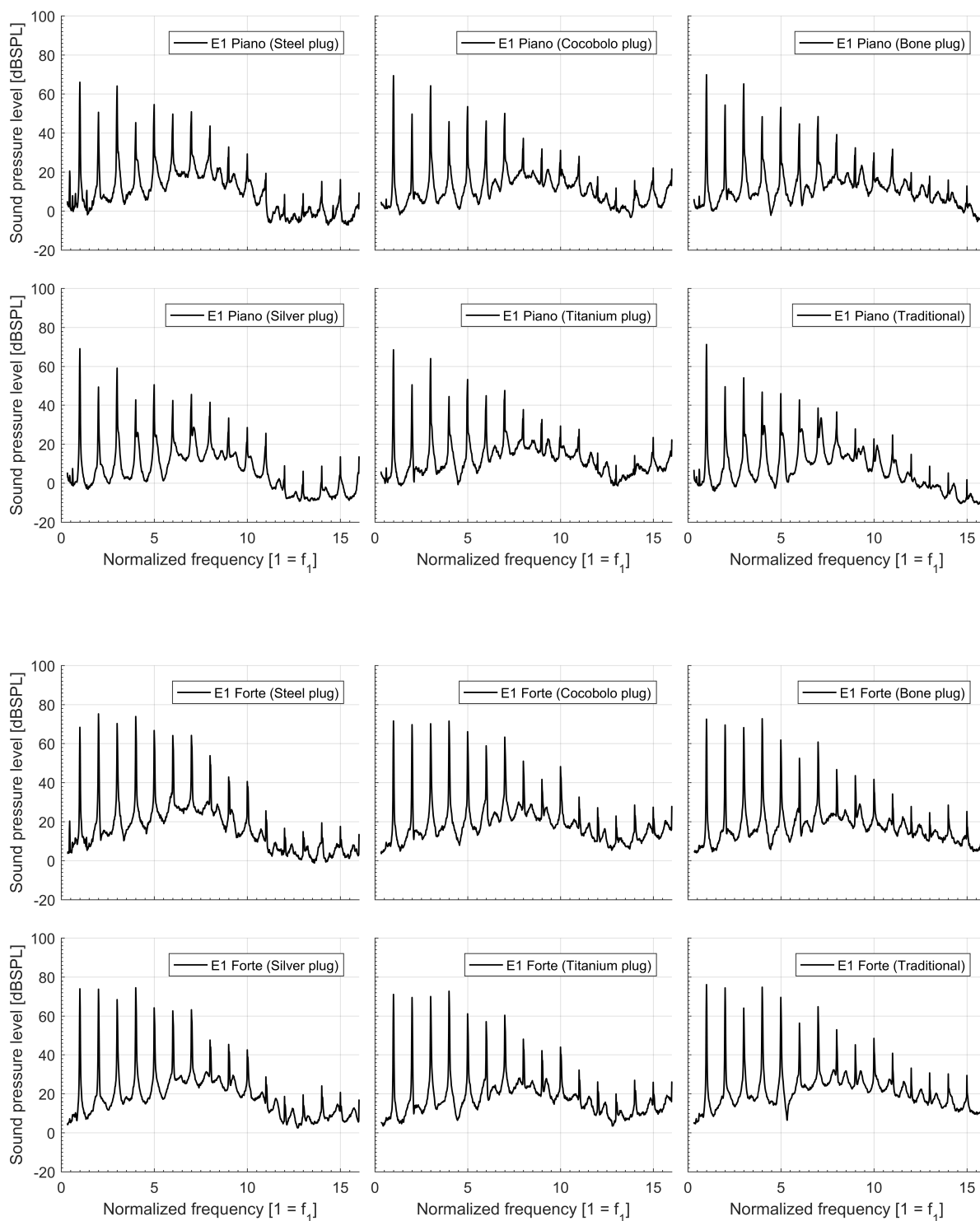


Figure 11: Steady state spectrum of the note E1 played with *piano* (first and second rows) and *forte* (third and fourth rows) dynamics on flutes with different head joints. (All diagrams have the same scale and shows the spectrum measured at the open end of the flute.)

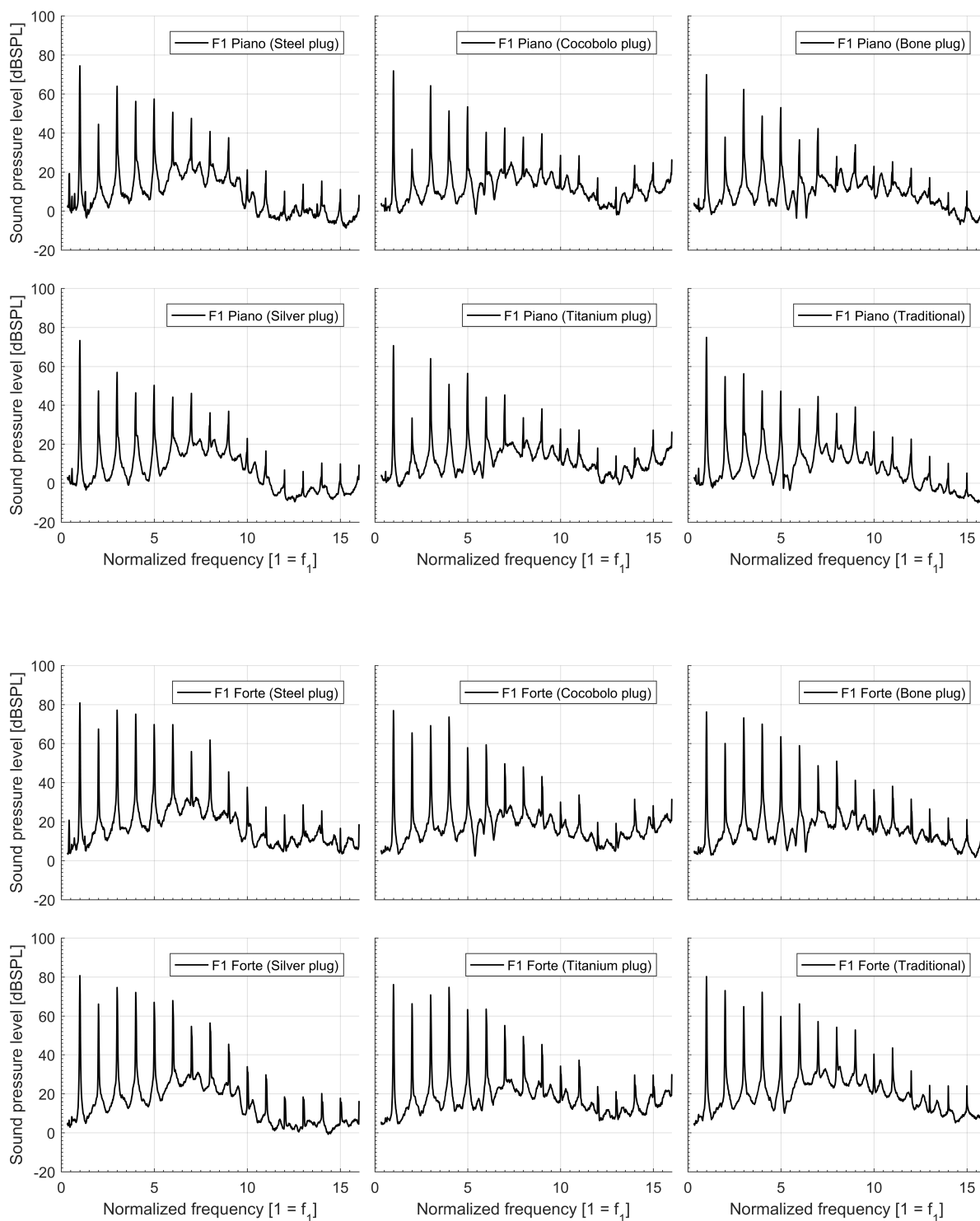


Figure 12: Steady state spectrum of the note F1 played with *piano* (first and second rows) and *forte* (third and fourth rows) dynamics on flutes with different head joints. (All diagrams have the same scale and shows the spectrum measured at the open end of the flute.)

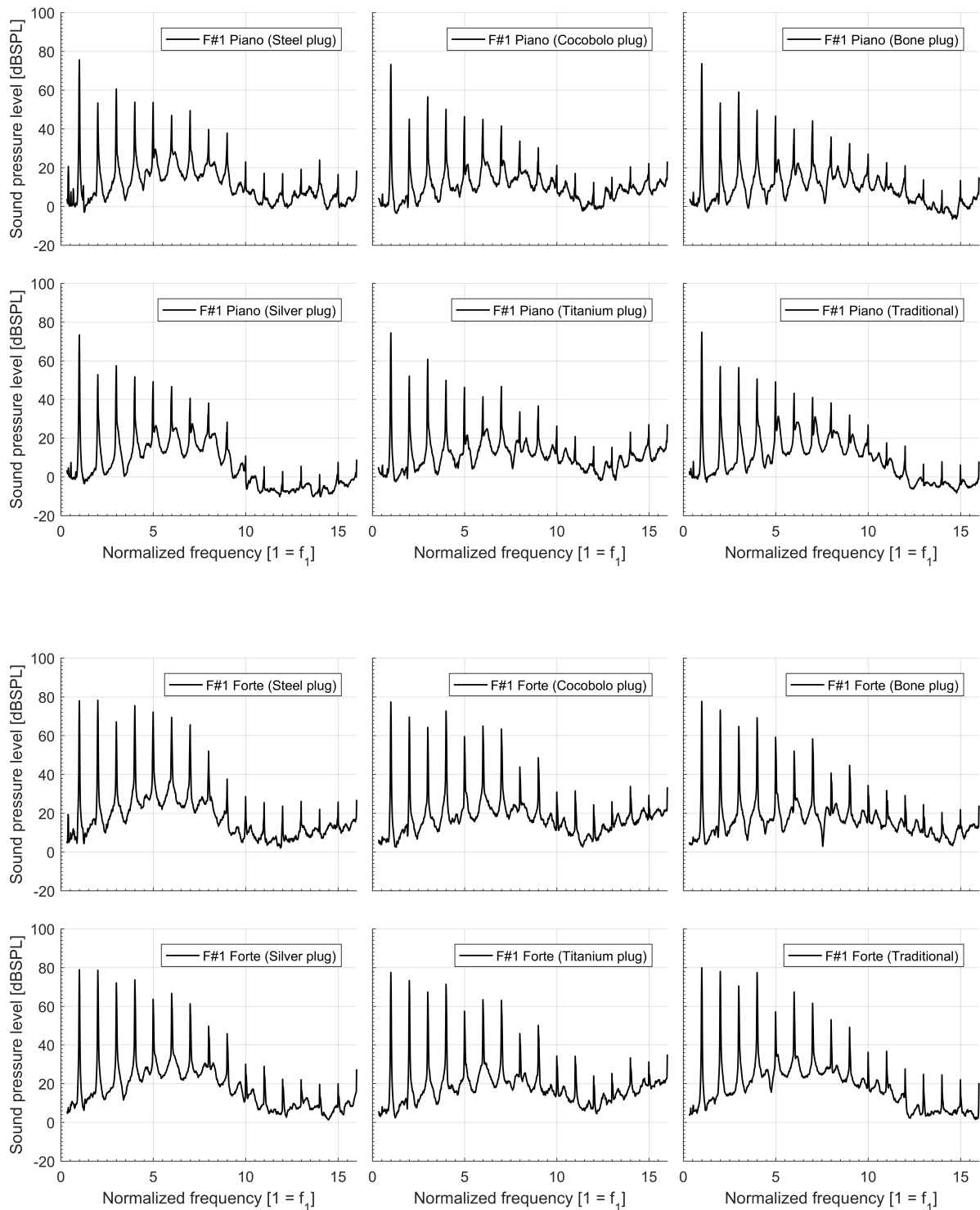


Figure 13: Steady state spectrum of the note F#1 played with *piano* (first and second rows) and *forte* (third and fourth rows) dynamics on flutes with different head joints. (All diagrams have the same scale and shows the spectrum measured at the open end of the flute.)

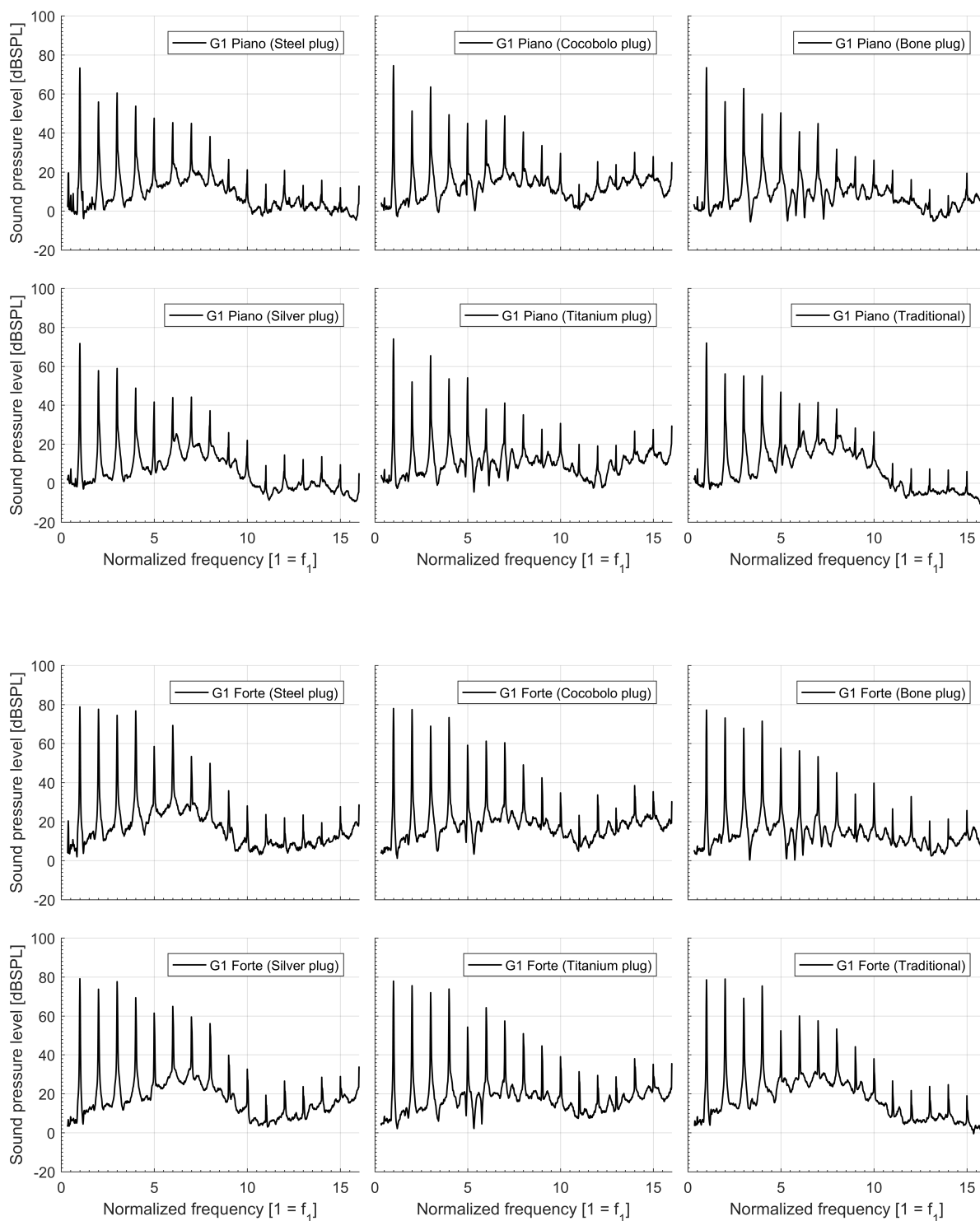


Figure 14: Steady state spectrum of the note G1 played with *piano* (first and second rows) and *forte* (third and fourth rows) dynamics on flutes with different head joints. (All diagrams have the same scale and shows the spectrum measured at the open end of the flute.)

3.5 Evaluation of vibration levels

Similar to the analysis of steady state sound pressure spectra, the steady state vibration acceleration spectra were also calculated. Measured acceleration levels are shown in Figure 15, in case of note G1. In the lower register similar vibration spectra were attained in case of other tones too. Comparing with Figure 14, it is observed that the vibration acceleration spectrum is significantly different from the spectrum of the radiated sound. When playing the notes with *piano* dynamics, the amplitude difference between the first three harmonics is much less in case of the acceleration signal, than that for the radiated sound. In case of *forte* dynamics it is observed that the octave is by far the strongest component in the acceleration spectra, while in the radiated sound the fundamental and the octave have very similar amplitudes.

Comparing vibration levels the following conclusion can be drawn. The greatest difference of average levels between the conventional and reform flute heads is 3 dB in the lower register with *piano* dynamics, and 6 dB in the middle register with *forte* dynamics.

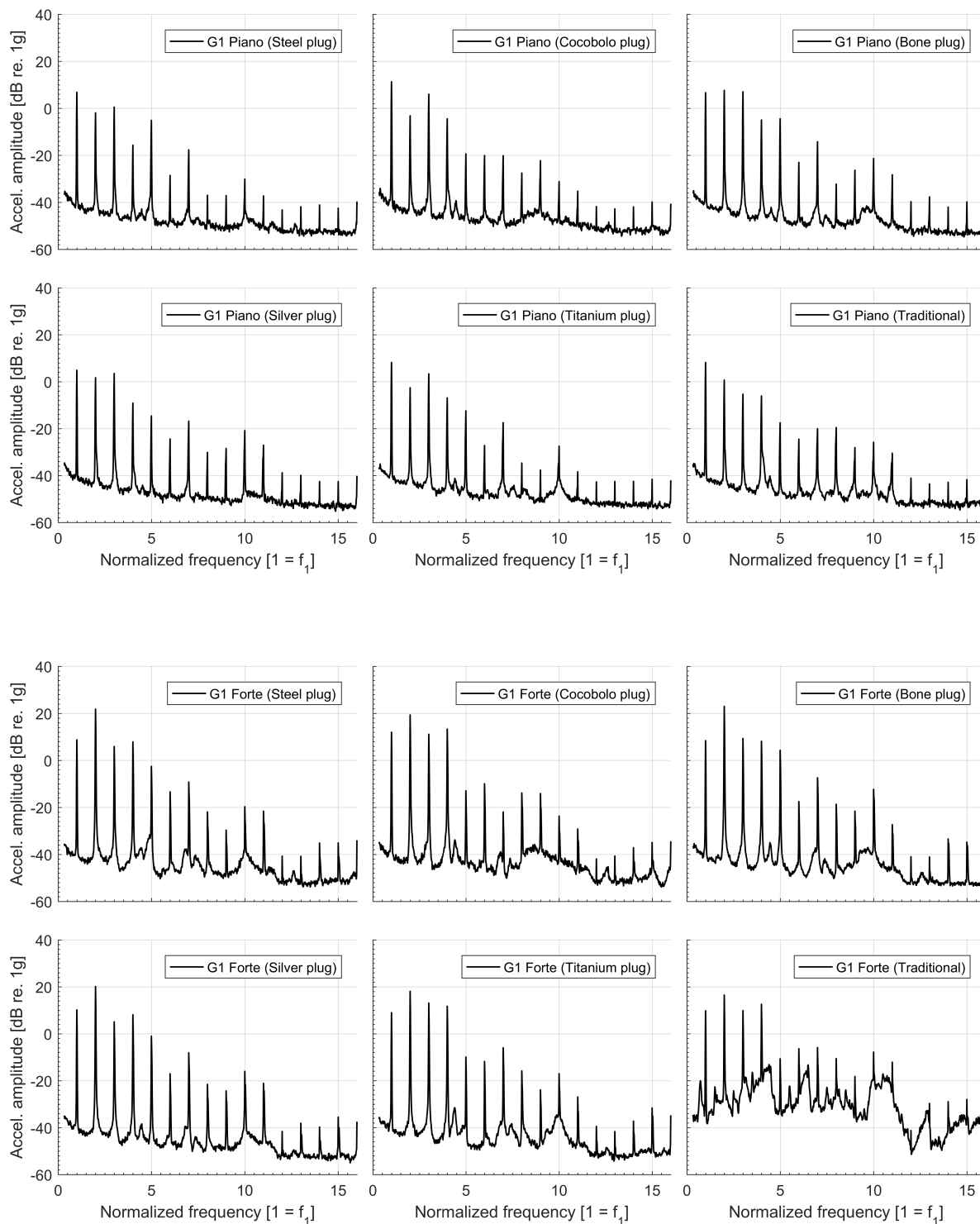


Figure 15: Acceleration amplitude in case of the note G1 measured near the open end of the flute with *piano* (first and second rows) and *forte* (third and fourth rows) dynamics on different flute sets. (All diagrams have the same scale.)

4 Analysis of the attack phase

In order to investigate how notes are started, the attack phases of the sounds were analyzed. The attack phase plays an important role in the perceived quality of the sound, therefore it is worth analyzing the attack phase in an objective manner too. The attack phase is determined by the segmentation method described in Section 1.4. In the analysis the time history of the amplitudes of the harmonics are examined during the attack phase. Previous experiments on other types of musical instruments show that this examination should be carried out on the signal recorded by the microphone placed close to the embouchure. This is also supported by the fact that the attack of the sound is strongly influenced by the blowing strength. Thus, the effect can be best measured near the embouchure hole.

In order to identify the harmonic components in the spectra, the attack phases were resampled based on the fundamental frequency f_1 extracted from the consecutive steady state phase. This makes the precise calculation of the amplitude of the harmonics possible even with using a small window size. The latter is necessary to attain a fine temporal resolution. The following parameters were used: resampling frequency $f'_s = 64f_1$, window size $N_{\text{win}} = 256$, overlapping of successive time windows : $7/8$. This way, 2 time windows start in each period of the sound, and the time resolution becomes $\Delta t = 1/(2f_1)$.

It is a general feature of wind instruments that the attacks are slightly different when the same note is played repeatedly. These differences are also observable when air is supplied to the instrument by a controlled mechanical system (e.g. the wind system in case of pipe organs). When notes are played on a flute, these differences are natural as the air is supplied by the flautist. However, this human interaction renders the objective evaluation of the attack phase more difficult. During the analysis the following was observed. There is a significant difference in the attacks of the notes of the lower and the middle register (which are considered to be much easier to play) and the notes of the upper register especially with *piano* dynamics (which are considered to be more difficult to play). While the attacks of successive notes in the lower and middle registers are very much alike, in case of more difficult notes a greater variation of the attacks was observed. This phenomenon is illustrated in Figure 3 above. Therefore, in the subsequent figures always the fastest attack (from the three consecutive ones) is shown as this can be regarded as the “smoothest” one.

Figures 16 and 17 show the attack phases of the notes F#1 and G1, respectively. The diagrams display the time histories of the amplitudes of the first five harmonic partials in the sound. All diagrams have the same scale and the unit of the normalized time is the period corresponding to the fundamental frequency. The chosen notes (F#1 and G1) represent the phenomena observed in the lower register quite well. The investigation showed that notes played with *forte* dynamics start much faster than the same notes played with *piano* dynamics. The greatest difference between the novel flute heads and the traditional one is observed in case of the note F#1. With *piano* dynamics the attack is much slower with the traditional head than with any of the new heads. With the conventional head, in case of either dynamics (*piano* and *forte*) the fifth harmonic (major third) appears with a great amplitude in the beginning of the attack phase. This unique phenomenon was not observed neither when playing the same note with any of the new flute heads or when playing the neighbouring F1 or G1 notes.

Beside the speed of the attack the strength of the harmonics in the attack phase are also influenced by the flute head. For example, in case of the note F#1 played with *forte* dynamics, it is observable that when played with the steel, bone or silver plug, the third harmonic (pure fifth) appears the fastest. With cocobolo and titanium plugs, the octave is faster than the fifth. In case of the conventional plug, the octave and fifth are built up simultaneously.

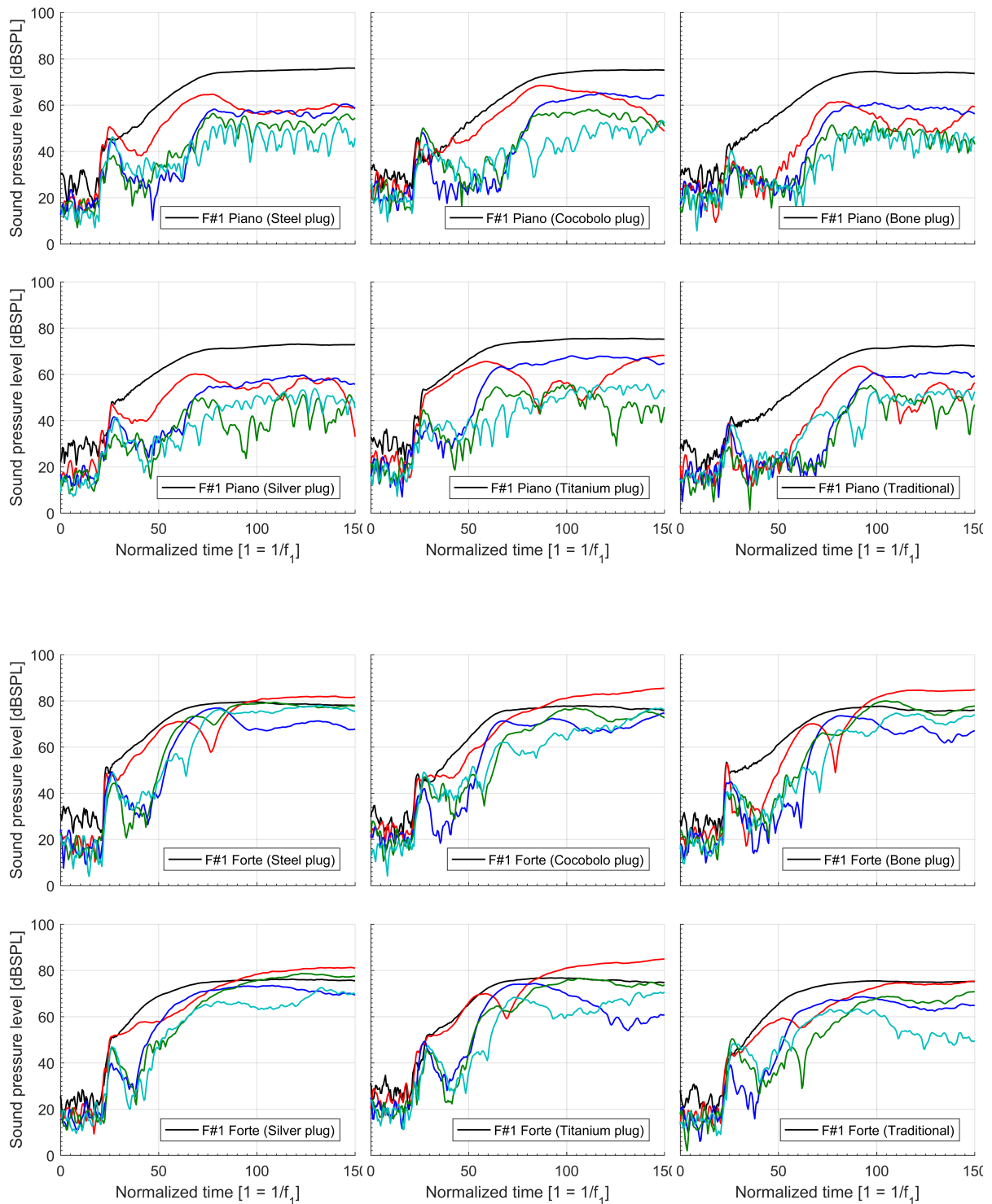


Figure 16: Attack of the note F#1 played with *piano* (first and second rows) and *forte* (third and fourth rows) dynamics on the flutes equipped with different tuning plugs. The colors show the harmonics in each chart: black – fundamental, red – octave, blue – pure fifth, green – second octave, turquoise – major third. (All diagrams have the same scale and shows the levels measured by the microphone close to the embouchure.)

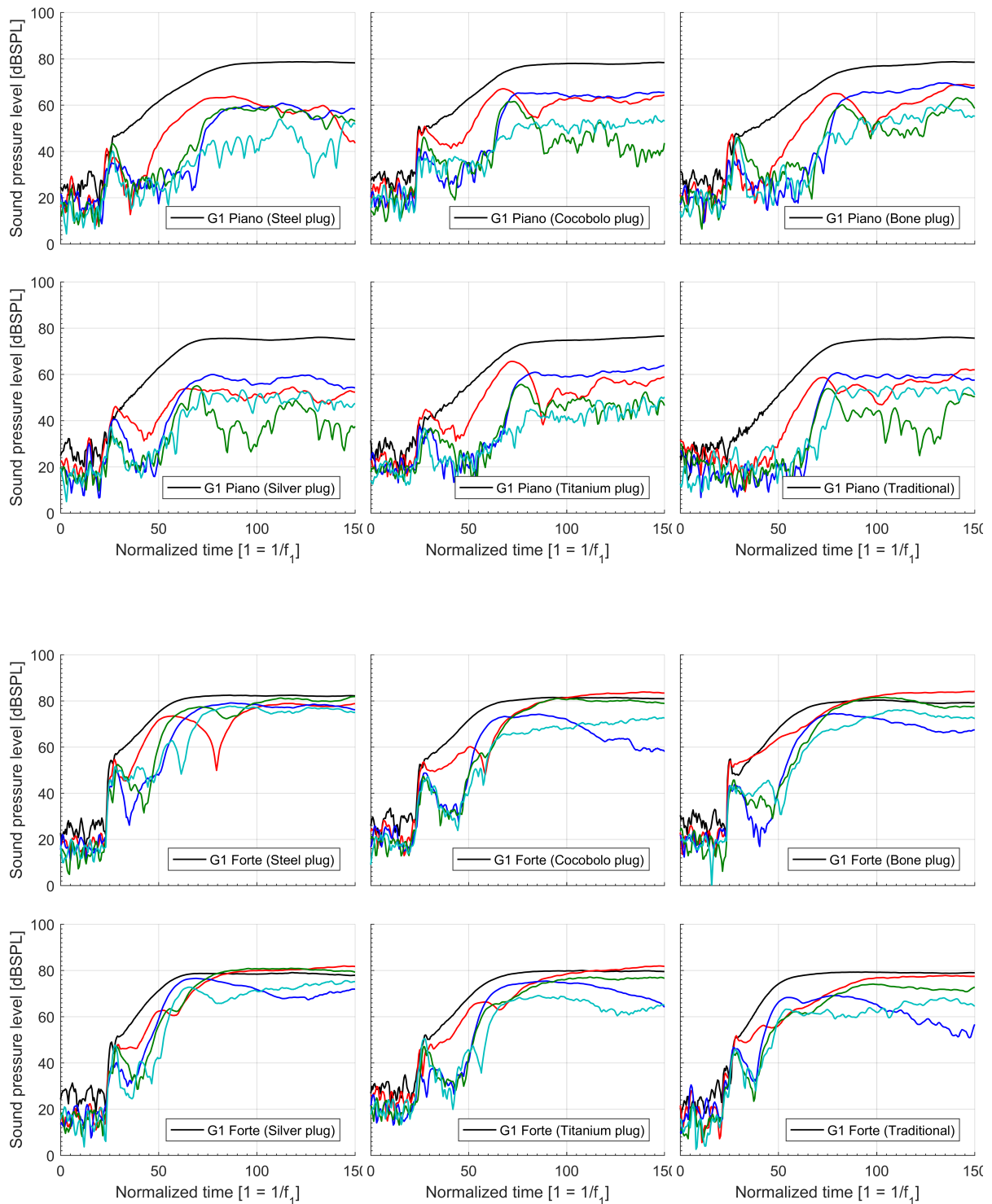


Figure 17: Attack of the note G1 played with *piano* (first and second rows) and *forte* (third and fourth rows) dynamics on the flutes equipped with different tuning plugs. The colors show the harmonics in each chart: black – fundamental, red – octave, blue – pure fifth, green – second octave, turquoise – major third. (All diagrams have the same scale and shows the levels measured by the microphone close to the embouchure.)

5 Evaluation of the results

Based on the findings described above, the following conclusions can be made.

1. The spectral centroid of the steady state sounds becomes higher with applying the new head joints. This phenomenon is visualized in Figure 6 and described quantitatively in the data of Table 2. Thus, the flute can produce a sound that is richer in higher harmonics by applying any of the novel head joints. This statement is also confirmed by the spectra visualized in Figures 7–14.
2. There are significant differences between the sound spectra of the held notes produced by the conventional flute and by the flute equipped with any of the improved head joints. This is visible in the charts of Figures 7–14. It is observed especially in the lower register that the envelopes of the spectra are also significantly different from that of the traditional spectrum. For example when examining the note E1, it can be observed that the strongest component of the note is the fundamental harmonic in case of a conventional flute. When the same note is played with any of the new head joints, the first and the second octave will have the same or stronger amplitude as the fundamental harmonic. Similar phenomena were found when analyzing further notes of the musical scale, which were not discussed in this report. It can be assumed that these objective differences can also be heard when listening to the different sounds.
3. Spectra recorded by accelerometer sensors show significant differences for the different flute heads. How these observed differences influence the perceived sound quality was not a subject of our investigations, therefore this question is left open.
4. There are also significant differences between the various flute sets in the attack of the sound. Regarding the speed of the attacks, these differences are in favour of the new flute heads. Also the head joint has a strong influence on the sequence of appearance and the strength of the harmonics in the attack phase.

Based on the above results it can be assessed that the measurement and analysis methods presented above can successfully be applied for evaluating objective qualities of flute sounds. Finally, it can be stated that there are quantifiable differences between the sounds produced by the conventional and the innovative flute heads.

Budapest, 28 April 2017

.....
Péter Rucz